ISSN 2347-3487

Effects of MHD and wall properties on the peristaltic transport of a Carreau fluid through porous medium

Dheia G. Salih Al-Khafajy[1], Ahmed M. Abdulhadi[2]

[1] Department of Mathematics, College of Computer Science and Mathematics, University of Al-Qadissiya, Diwaniya-Iraq. E-mail: dr.dheia.g.salih@gmail.com

[2] Department of Mathematics, College of Science, University of Baghdad, Baghdad-Iraq. E-mail: ahm6161@yahoo.com

ABSTRACT

This work concerns the peristaltic flow of a Carreau fluid model through porous medium under combined effects of MHD and wall properties. The assumptions of Reynolds number and long wavelength is investigated. The flow is investigated in a wave frame of reference moving with velocity of the wave. The perturbation series in terms of the Weissenberg number (We <1) was used to obtain explicit forms for velocity field and stream function. The effects of thermal conductivity, Grashof number, Darcy number, magnet, rigidity, stiffness of the wall and viscous damping force parameters on velocity, temperature and stream function have been studied.

Keywords

MHD; Peristaltic transport; Carreau fluid; Porous medium.

Council for Innovative Research

Peer Review Research Publishing System

Journal: JOURNAL OF ADVANCES IN PHYSICS

Vol. 6, No.2

www.cirjap.com, japeditor@gmail.com

ISSN 2347-3487

1. INTRODUCTION

Peristaltic flows have attracted the interest of a number of researchers because of wide applications in physiology and industry. The word peristaltic comes from a Greek word Peristaltikos which means clasping and compressing. The peristaltic transport is traveling contraction wave along a tube-like structure, and it results physiologically from neuron-muscular properties of any tubular smooth muscle. Peristaltic motion of blood in animal or human bodies has been considered by many authors. It is an important mechanism for transporting blood, where the cross-section of the artery is contracted or expanded periodically by the propagation of progressive wave. It plays an indispensable role in transporting many physiological fluids in the body in various situations such as urine transport from the kidney to the bladder through the ureter, transport of spermatozoa in the ducts efferentes of the male reproductive tract and the movement of ovum in the fallopin tubes. Roller and finger pumps using viscous fluids also operate on this principle, gastro-intestinal tract, bile ducts and other glandular ducts. The principle of peristaltic transport has been exploited for industrial applications like sanitary fluid transport, blood pumps in heart lungs machine and transport of corrosive fluids where the contact of the fluid with the machinery parts is prohibited. Since the first investigation of Latham [1] and Shapiro et al. [2] extensive analytical studies have been undertaken which involve such fluids. Important studies to the topic include the works in [3-11].

Investigation of flow through a porous medium has many applications in various branches of science and technology. The applications in which flow through a porous medium is mostly prominent are filtration of fluids, seepage of water in river beds, movement of underground water and oils, limestone, wood, the human lung, bile duct, gallbladder with stones, and small blood vessels which are few examples of flow through porous medium [12]. Pandey and Chaube [13] have examined the peristaltic flow of micropolar fluid through a porous medium in the presence of external magnetic field. They pointed out that the maximum pressure is strongly dependent on permeability of porous medium. Reddy et al. [14] have recently given the idea that the sagittal cross-section of the uterus may be better approximated by a tube of rectangular cross-section than a two-dimensional channel and presented the influence of lateral walls on peristaltic flow in a rectangular duct. Reddy et al. [15] studied the effect of thickness of the porous material on the peristaltic pumping when the tube wall is provided with non-erodible porous lining. Lakshminarayana et al. [16] studied the peristaltic pumping of a conducting fluid in a channel with a porous peripheral layer. Radhakrishnamacharya and Srinivasulu [17] studied the influence of wall properties on peristaltic transport with heat transfer.

Magnetohydrodynamic (MHD) peristaltic flows have acquired a lot of credence due to their applications. The effects of MHD on the peristaltic flow of Newtonian and non-Newtonian fluids for different geometries have been discussed by many researchers [18-21], with a view to understand some practical phenomena such as blood pump machine and Magnetic Resonance Imaging (MRI) which is used for diagnosis of brain, vascular diseases and all the human body. In the studies [18-21], the uniform MHD has been used. There are a few attempts in which induced magnetic field is used. They are mentioned in the works of [22-30]. Rathod et al. [31] studied the influence of wall properties on MHD peristaltic transport of dusty fluid. A new model for study the effect of wall properties on peristaltic transport of a viscous fluid has been investigated by Mokhtar and Haroun [32], Srinivas et al. [33] studied the effect of slip, wall properties and heat transfer on MHD peristaltic transport. Sreenadh et al. [34] studied the effects of wall properties and heat transfer on the peristaltic transport of food bolus through oesophagus. Al-Khafajy and Abdulhadi [35] analyzed the Effects of MHD and wall properties on the peristaltic transport of a Jeffrey fluid through porous medium channel.

Ali et al. [36] presented the analytic solution of the mathematical modeling for the flow of incompressible Carreau fluid in an asymmetric channel with sinusoidal wall variations. Hayat et al. [37] examined the MHD peristaltic flow of a Carreau fluid in a channel with different waveforms. Due to the non-linear dependence, the analysis of the behaviors of the non-Newtonian Carreau fluids tends to be more complicated and subtle in comparison with that of the non-Newtonian fluids. In general, the equations of motion for non-Newtonian fluids are of higher complexity than the Navier-Stokes equations and thus one needs some conditions in addition to the usual adherence boundary condition. Hence, there is a need for a method which provides a means of obtaining other conditions necessary for the solution.

Motivated by this, we consider a mathematical model to study the peristaltic flow of a Carreau fluid under the effect of MHD and wall properties through porous medium. In the laboratory frame under the assumptions of long wavelength and low Reynolds number, the solutions of the governing equations of Carreau fluid have been found by using perturbation method. The results are analyzed for different values of parameters namely Grashof number, Darcy number, thermal conductivity, magnet, rigidity, stiffness and viscous damping forces of the channel wall.

2. MATHEMATICAL FORMULATION

Consider the peristaltic flow of an incompressible Carreau fluid in a flexible channel with flexible induced by sinusoidal wave trains propagating with constant speed c along the channel walls.

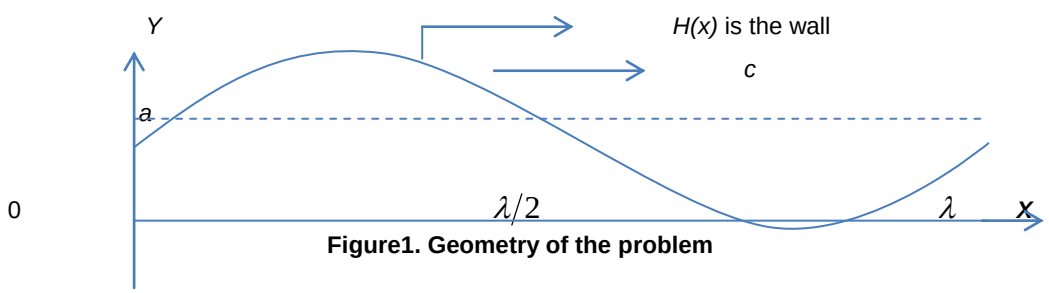

Figure1. Geometry of the problem

ISSN 2347-3487

The wall deformation is given by

$$H(\bar{x},\bar{t}) = a - \bar{\phi}\cos^2\frac{\pi}{\lambda}(\bar{x} - c\bar{t}) \quad (1)$$

where $\bar{h}$, $\bar{x}$, $\bar{t}$, $\bar{\phi}$, λ and *c* represent transverse vibration of the wall, axial coordinate, time, half width of the channel, amplitude of the wave, wavelength and wave velocity respectively.

The constitutive equation for a Carreau fluid [38] is

$$\bar{\tau} = -[\mu_\infty + (\mu_0 - \mu_\infty)\left(1 + (\Gamma\bar{\dot{\gamma}})^2\right)^{\frac{n-1}{2}}]\bar{\dot{\gamma}} \quad (2)$$

where τ is the extra stress tensor, μ_∞ is the infinite shear rate viscosity, μ_0 is the zero shear rate viscosity, Γ is the time constant, *n* is the dimensionless power law index and $\dot{\gamma}$ is defined as

$$\dot{\gamma} = \sqrt{\frac{1}{2}\sum_i\sum_j \dot{\gamma}_{ij}\dot{\gamma}_{ji}} = \sqrt{\frac{1}{2}\Pi} \quad (3)$$

Here Π is the second invariant stress tensor. We consider in the constitutive equation (2) the case for which μ_∞ = 0 and $\Gamma\dot{\gamma}$ < 1 so we can write

$$\bar{\tau} = -\mu_0[1 + \frac{n-1}{2}(\Gamma\bar{\dot{\gamma}})^2]\bar{\dot{\gamma}} \quad (4)$$

The above model reduces to Newtonian model for *n* = 1 or Γ = 0.

The basic equations governing the non-Newtonian incompressible Carreau fluid are given by:

The continuity equation is given by:

$$\frac{\partial\bar{u}}{\partial\bar{x}} + \frac{\partial\bar{v}}{\partial\bar{y}} = 0, \quad (5)$$

The momentum equations are:

$$\rho(\frac{\partial\bar{u}}{\partial\bar{t}} + \bar{u}\frac{\partial\bar{u}}{\partial\bar{x}} + \bar{v}\frac{\partial\bar{u}}{\partial\bar{y}}) = -\frac{\partial\bar{p}}{\partial\bar{x}} + \frac{\partial\bar{\tau}_{\bar{x}\bar{x}}}{\partial\bar{x}} + \frac{\partial\bar{\tau}_{\bar{x}\bar{y}}}{\partial\bar{y}} + \rho g\alpha(T - T_0) - \sigma B_0^2\bar{u} - \frac{\mu_0}{k}\bar{u}, \quad (6)$$

$$\rho(\frac{\partial\bar{v}}{\partial\bar{t}} + \bar{u}\frac{\partial\bar{v}}{\partial\bar{x}} + \bar{v}\frac{\partial\bar{v}}{\partial\bar{y}}) = -\frac{\partial\bar{p}}{\partial\bar{y}} + \frac{\partial\bar{\tau}_{\bar{y}\bar{x}}}{\partial\bar{x}} + \frac{\partial\bar{\tau}_{\bar{y}\bar{y}}}{\partial\bar{y}} - \frac{\mu_0}{k}\bar{v} \quad (7)$$

The temperature equation is given by:

$$\rho(\frac{\partial T}{\partial\bar{t}} + \bar{u}\frac{\partial T}{\partial\bar{x}} + \bar{v}\frac{\partial T}{\partial\bar{y}}) = \frac{k}{c_p}(\frac{\partial^2 T}{\partial\bar{x}^2} + \frac{\partial^2 T}{\partial\bar{y}^2}) + \Phi, \quad (8)$$

where $\bar{u}$ is the axial velocity, $\bar{v}$ transverse velocity, $\bar{y}$ transverse coordinate, ρ fluid density, $\bar{p}$ pressure, μ_0 fluid viscosity, g acceleration due to gravity, α coefficient of linear thermal expansion of fluid, B_0 magnetic parameter, *T* temperature, c_p specific heat at constant pressure, *k* is the thermal conductivity and Φ constant heat addition/absorption.

The velocity and temperatures at the central line and the wall of the peristaltic channel are given as:

$T = T_0$ at $\bar{y} = 0$

$T = T_1$ at $\bar{y} = \bar{h}$

where T_0 is the temperature at centre is line and T_1 is the temperature on the wall of peristaltic channel.

The governing equation of motion of the flexible wall may be expressed as:

$$L^* = \bar{p} - \bar{p}_0 \tag{9}$$

where L^* is an operator, which is used to represent the motion of stretched membrane with viscosity damping forces such that

$$L^* = -\kappa \frac{\partial^2}{\partial x^2} + m_1 \frac{\partial^2}{\partial t^2} + C \frac{\partial}{\partial t} \tag{10}$$

where κ is the elastic tension in the membrane, m_1 is the mass per unit area, *C* is the coefficient of viscous damping forces.

Continuity of stress at $y = \bar{h}$ and using momentum equation, yield

$$\frac{\partial}{\partial \bar{x}} L^*(\bar{h}) = \frac{\partial \bar{p}}{\partial \bar{x}} = \frac{\partial \bar{\tau}_{\bar{x}\bar{x}}}{\partial \bar{x}} + \frac{\partial \bar{\tau}_{\bar{x}\bar{y}}}{\partial \bar{y}} - \rho\left(\frac{\partial \bar{u}}{\partial \bar{t}} + \bar{u}\frac{\partial \bar{u}}{\partial \bar{x}} + \bar{v}\frac{\partial \bar{u}}{\partial \bar{y}}\right) + \rho g \alpha (T - T_0) - \sigma B_0^2 \bar{u} - \frac{\mu_0}{k}\bar{u} \tag{11}$$

In order to simplify the governing equations of the motion, we may introduce the following dimensionless transformations as follows:

$$\left.\begin{aligned} &x = \frac{\bar{x}}{\lambda}, y = \frac{\bar{y}}{a}, \delta = \frac{a}{\lambda}, u = \frac{\bar{u}}{c}, v = \frac{\bar{v}}{c\delta}, t = \frac{c\bar{t}}{\lambda}, \phi = \frac{\bar{\phi}}{a}, We = \frac{\Gamma c}{a}, Da = \frac{k}{a^2}, \\ &p = \frac{a^2 \bar{p}}{\mu_0 \lambda c}, Gr = \frac{gpa^2 \alpha (T_1 - T_0)}{c\mu_0^{\ 2}}, \theta = \frac{T - T_0}{T_1 - T_0}, M^2 = \frac{\sigma B_0^2 a^2}{\mu_0}, \beta = \frac{a^2 \Phi}{k(T_1 - T_0)}, \\ &\mathrm{Re} = \frac{\rho c a}{\mu_0}, \mathrm{Pr} = \frac{\mu_0 c_p}{k}, \tau_{xx} = \frac{\lambda}{\mu_0 c}\bar{\tau}_{\bar{x}\bar{x}}, \tau_{xy} = \frac{a}{\mu_0 c}\bar{\tau}_{\bar{x}\bar{y}}, \tau_{yy} = \frac{\lambda}{\mu_0 c}\bar{\tau}_{\bar{y}\bar{y}}, \dot{\gamma} = \frac{a\bar{\dot{\gamma}}}{c} \end{aligned}\right\} \tag{12}$$

where δ is the length of the channel, *We* Weissenberg number, *Da* Darcy number, Re Reynolds number, *Gr* Grashof number, θ dimensionless temperature, M magnetic parameter, β dimensionless heat source/sink parameter and Pr Prandtl number.

Substituting (12) into equations (1)-(11), we obtain the following non-dimensional equations and boundary conditions:

$$h(x,t) = 1 - \phi \cos^2 \pi (x - t) \tag{13}$$

$$\frac{\partial u}{\partial x} + \frac{\partial v}{\partial y} = 0 \tag{14}$$

$$\mathrm{Re}\,\delta\left(\frac{\partial u}{\partial t} + u\frac{\partial u}{\partial x} + v\frac{\partial u}{\partial y}\right) = -\frac{\partial p}{\partial x} + \delta^2 \frac{\partial \tau_{xx}}{\partial x} + \frac{\partial \tau_{xy}}{\partial y} + \frac{\rho g a^2 \alpha (T - T_0)}{\mu_0 c}\theta - M^2 u - \frac{1}{Da}u \tag{15}$$

$$\mathrm{Re}\,\delta^3\left(\frac{\partial v}{\partial t} + u\frac{\partial v}{\partial x} + v\frac{\partial v}{\partial y}\right) = -\frac{\partial p}{\partial x} + \delta^2\left(\frac{\partial \tau_{yx}}{\partial x} + \frac{\partial \tau_{yy}}{\partial y}\right) - \frac{\delta^2}{Da}v \tag{16}$$

$$\frac{\mathrm{Re}\,\delta\,\mathrm{Pr}}{(T_1 - T_0)}\left(\frac{\partial}{\partial t} + u\frac{\partial}{\partial x} + v\frac{\partial}{\partial y}\right)(\theta(T_1 - T_0) + T_0) = \delta^2 \frac{\partial^2 \theta}{\partial x^2} + \frac{\partial^2 \theta}{\partial y^2} + \beta \tag{17}$$

$$\delta^2 \frac{\partial \tau_{xx}}{\partial x} + \frac{\partial \tau_{xy}}{\partial y} + Gr\theta - \left(M^2 + \frac{1}{Da}\right)u - \mathrm{Re}\,\delta\left(\frac{\partial u}{\partial t} + u\frac{\partial u}{\partial x} + v\frac{\partial u}{\partial y}\right) = E_1 \frac{\partial^3 h}{\partial x^3} + E_2 \frac{\partial^3 h}{\partial x \partial t^2} + E_3 \frac{\partial^2 h}{\partial x \partial t} \tag{18}$$

where

ISSN 2347-3487

$$\left.\begin{aligned}
\tau_{xx} &= -2[1+\frac{(n-1)}{2}We^2\dot{\gamma}^2]\frac{\partial u}{\partial x}\\
\tau_{xy} &= -[1+\frac{(n-1)}{2}We^2\dot{\gamma}^2]\left(\frac{\partial u}{\partial y}+\delta^2\frac{\partial v}{\partial x}\right)\\
\tau_{yy} &= -2[1+\frac{(n-1)}{2}We^2\dot{\gamma}^2]\frac{\partial v}{\partial y}\\
\dot{\gamma} &= \sqrt{2\delta^2\left(\left(\frac{\partial u}{\partial x}\right)^2+\left(\frac{\partial v}{\partial y}\right)^2\right)+\left(\frac{\partial u}{\partial y}+\delta^2\frac{\partial v}{\partial x}\right)^2}
\end{aligned}\right\} \quad (19)$$

The corresponding boundary conditions are

$\frac{\partial u}{\partial y} = 0$ at $y = 0$ (the regularity condition) (20)

$u = 0$ at $y = h$ (the no slip condition) (21)

$v = 0$ at $y = 0$ (the absence of transverse velocity) (22)

$\theta = 0$ at $y = 0$ and $\theta = 1$ at $y = h$ (23)

3. SOLUTION OF THE PROBLEM

The general solution of the governing equations (14)-(18) in the general case seems to be impossible; therefore, we shall confine the analysis under the assumption of small dimensionless wave number. It follows that δ << 1. In other words, we considered the long-wavelength approximation. Along to this assumption, equations (13)-(18) become:

$$h(x,t) = 1-\phi\cos^2\pi(x-t)$$

(24) $$\frac{\partial u}{\partial x}+\frac{\partial v}{\partial y}=0$$

(25) $$\frac{\partial p}{\partial x}=\frac{\partial}{\partial y}\left(-\left[1+\frac{(n-1)}{2}We^2\left(\frac{\partial u}{\partial y}\right)^2\right]\frac{\partial u}{\partial y}\right)+Gr\theta-(M^2+\frac{1}{Da})u$$

(26) $$\frac{\partial p}{\partial y}=0$$

(27) $$\frac{\partial^2\theta}{\partial y^2}+\beta=0$$

(28) $$\frac{\partial}{\partial y}\left(-\left[1+\frac{(n-1)}{2}We^2\left(\frac{\partial u}{\partial y}\right)^2\right]\frac{\partial u}{\partial y}\right)+Gr\theta-(M^2+\frac{1}{Da})u=E_1\frac{\partial^3 h}{\partial x^3}+E_2\frac{\partial^3 h}{\partial x\partial t^2}+E_3\frac{\partial^2 h}{\partial x\partial t}$$

(29) The corresponding Stream function ($u=\partial\psi/\partial y$, $v=-\partial\psi/\partial x$) with boundary condition $\psi=0$ at $y=0$.

The exact solution of equation (28) with boundary condition equation (23) is

$$\theta=\frac{y}{h}+\frac{\beta}{2}(hy-y^2)$$

(30) Equation (27) shows that p dependents on *x* only. Equation (29) is non-linear and it is difficult to get a closed form solution. However for vanishing *We*, the boundary value problem is agreeable to an easy analytical solution. In this case the equation becomes linear and can be solved. Nevertheless, small Γ suggests the use of perturbation technique to solve the non-linear problem. Accordingly, we write

ISSN 2347-3487

$$\left.\begin{aligned} u &= u_0 + We^2 u_1 + We^4 u_2 + O(We^6) \\ \psi &= \psi_0 + We^2 \psi_1 + We^4 \psi_2 + O(We^6) \end{aligned}\right\} \quad (31)$$

Substituting equations (31) into equation (29) with boundary conditions (20) and (21), then equating the like powers of *We*, we obtain

3.1 Zeroth-order system (We^0)

$$\frac{\partial^2 u_0}{\partial y^2} + (M^2 + \frac{1}{Da})u_0 - Gr\theta = E_1 \frac{\partial^3 h}{\partial x^3} + E_2 \frac{\partial^3 h}{\partial x \partial t^2} + E_3 \frac{\partial^2 h}{\partial x \partial t} \quad (32)$$

$$\psi_0 = \int u_0 dy \quad (33)$$

The associated boundary conditions are

$$\left.\frac{\partial u_0}{\partial y}\right|_{y=0} = u_0(h) = 0 \text{ and } \psi_0 = 0 \text{ at } y = 0 \quad (34)$$

3.2 First-order system (We^2)

$$\frac{\partial^2 u_1}{\partial y^2} + (M^2 + \frac{1}{Da})u_1 = -\frac{3(n-1)}{2}\left(\frac{\partial u_0}{\partial y}\right)^2 \left(\frac{\partial^2 u_0}{\partial y^2}\right) \quad (35)$$

$$\psi_1 = \int u_1 dy \quad (36)$$

The associated boundary conditions are

$$\left.\frac{\partial u_1}{\partial y}\right|_{y=0} = u_1(h) = 0 \text{ and } \psi_1 = 0 \text{ at } y = 0 \quad (37)$$

3.3 Second-order system (We^4)

$$\frac{\partial^2 u_2}{\partial y^2} + (M^2 + \frac{1}{Da})u_2 = -\frac{3(n-1)}{2}\left[\left(\frac{\partial u_0}{\partial y}\right)^2 \left(\frac{\partial^2 u_1}{\partial y^2}\right) + 2\left(\frac{\partial^2 u_0}{\partial y^2}\right)\left(\frac{\partial u_1}{\partial y}\right)\left(\frac{\partial u_0}{\partial y}\right)\right] \quad (38)$$

$$\psi_2 = \int u_2 dy \quad (39)$$

The associated boundary conditions are

$$\left.\frac{\partial u_2}{\partial y}\right|_{y=0} = u_{21}(h) = 0 \text{ and } \psi_2 = 0 \text{ at } y = 0 \quad (40)$$

3.4 Zeroth-order solution

The solutions of equations (32) and (33) subset to the associates boundary conditions (34) are found to be of the form;

$$u_0 = D_1.\cos(y\sqrt{A_1}) + D_2.\sin(y\sqrt{A_1}) + \frac{Gr}{A_1^2 h}(yA_1 + h\beta) + \frac{y\beta Gr}{2A_1}(h-y) + \frac{2\pi^2\phi}{A_1}[2(E_1+E_2)\pi Sin(2\pi(x-t)) + E_3 Cos(2\pi(x-t))] \quad (41)$$

$$\psi_0 = \frac{1}{\sqrt{A_1}}\left(D_1.\sin(y\sqrt{A_1}) - D_2.\cos(y\sqrt{A_1}) + D_2\right) + \frac{Gr}{A_1^2 h}(\frac{1}{2}y^2 A_1 + yh\beta) + \frac{\beta Gr}{2A_1}(\frac{1}{2}y^2 h - \frac{1}{3}y^3) + \frac{2y\pi^2\phi}{A_1}[2(E_1+E_2)\pi Sin(2\pi(x-t)) + E_3 Cos(2\pi(x-t))] \quad (42)$$

where D_1 and D_2 are constants to be determinate by using the boundary conditions equation (34).

3.5 First-order solution

The solutions of equations (35) and (36) subset to the associates boundary conditions (37) are found to be of the form;

$$\psi_1 = -\frac{1}{192h^2A_1^5}\{3(n-1)A_1^{\frac{11}{2}}h^2[D_2^3 - 3D_1^2D_2] - 8(n-1)GrA_1^{\frac{7}{2}}h[-16h\beta D_1D_2 + 3(2+h^2\beta)\sqrt{A_1}(D_1^2 - D_2^2)] -$$

$$6A_1^{\frac{3}{2}}[6(n-1)Gr^2h\beta(2+h^2\beta)\sqrt{A_1}D_1 - 6(n-1)Gr^2h^2\beta^2D_2 + 9(n-1)(4+4h^2\beta+h^4\beta^2)Gr^2A_1D_2 + 9(n-1)$$

$$h^2A_1^4D_2(D_1^2+D_2^2) + 32h^2A_1^3D_4]\} + \frac{1}{192h^2A_1^5}\{576(1-n)Gr^3h^2\beta^3y + 288(n-1)Gr^3A_1\beta y + 288(n-1)$$

$$Gr^3h^2\beta^2A_1y + 288(1-n)Gr^3h\beta^2A_1y^2 - 72(1-n)Gr^3h^4\beta^3A_1y + 36(1-n)Gr^2h^2\beta^2A_1^{\frac{3}{2}}D_1\sin(y\sqrt{A_1})$$

$$+144(1-n)Gr^3h^3\beta^3A_1y^2 - 96(1-n)Gr^3h^2\beta^3A_1y^3 - 216(1-n)Gr^2A_1^{\frac{5}{2}}C_1\sin(y\sqrt{A_1}) - 216(1-n)\sin(y\sqrt{A_1})$$

$$Gr^2h^2\beta A_1^{\frac{5}{2}}D_1 + 144(1-n)Gr^2h\beta A_1^{\frac{5}{2}}D_1y.\sin(y\sqrt{A_1}) - 54(1-n)Gr^2h^4\beta^2A_1^{\frac{5}{2}}D_1.\sin(y\sqrt{A_1}) + 72(1-n)$$

$$Gr^2h^3\beta^2A_1^{\frac{5}{2}}D_1y.\sin(y\sqrt{A_1}) - 72(1-n)Gr^2h^2\beta^2A_1^{\frac{5}{2}}D_1y^2.\sin(y\sqrt{A_1}) + 64(1-n)Grh^2\beta A_1^{\frac{7}{2}}D_1^2.\sin(2y\sqrt{A_1})$$

$$-144(1-n)Grh^2\beta A_1^4D_1^2y - 54(1-n)h^2A_1^{\frac{11}{2}}D_1^3.\sin(y\sqrt{A_1}) - 3(1-n)h^2A_1^{\frac{11}{2}}D_1^3.\sin(3y\sqrt{A_1}) + 72(1-n)$$

$$Gr^2h\beta A_1^2D_2.\sin(y\sqrt{A_1}) + 36(1-n)Gr^2h^3\beta^2A_1^2D_2.\sin(y\sqrt{A_1}) - 72(1-n)Gr^2h^2\beta^2A_1^2D_2y.\sin(y\sqrt{A_1})$$

$$+144(1-n)Gr^2A_1^3D_2y.\sin(y\sqrt{A_1}) + 144(1-n)Gr^2h^2\beta A_1^3D_2y.\sin(y\sqrt{A_1}) - 144(1-n)Gr^2h\beta A_1^3D_2y^2$$

$$\sin(y\sqrt{A_1}) + 36(1-n)Gr^2h^4\beta^2A_1^3D_2y.\sin(y\sqrt{A_1}) - 72(1-n)Gr^2h^3\beta^2A_1^3D_2y^2.\sin(y\sqrt{A_1}) + 48(1-n)$$

$$Gr^2h^2\beta^2A_1^3D_2y^3.\sin(y\sqrt{A_1}) + 96(1-n)GrhA_1^4D_1D_2y.\sin(2y\sqrt{A_1}) + 48(1-n)Grh^3\beta A_1^4D_1D_2.\sin(2y\sqrt{A_1})$$

$$-96(1-n)Grh^2\beta A_1^4D_1D_2y.\sin(2y\sqrt{A_1}) + 9(1-n)h^2A_1^{\frac{11}{2}}D_1^2D_2.\cos(3y\sqrt{A_1}) + 36(1-n)h^2A_1^6D_1^2D_2y$$

$$\sin(y\sqrt{A_1}) - 64(1-n)Grh^2\beta A_1^{\frac{7}{2}}D_2^2.\sin(2y\sqrt{A_1}) - 144(1-n)Grh^2\beta A_1^4D_2^2y - 54(1-n)h^2A_1^{\frac{11}{2}}D_1D_2^2$$

$$\sin(2y\sqrt{A_1})+9(1-n)\,h^2A_1^{\frac{11}{2}}D_1D_2^2.\sin(3y\sqrt{A_1})-3(1-n)\,h^2A_1^{\frac{11}{2}}D_2^3.\cos(3y\sqrt{A_1})+36(1-n)\,h^2A_1^6D_2^3y$$

$$\sin(y\sqrt{A_1})+8(1-n)\,GrhA_1^{\frac{7}{2}}.\cos(2y\sqrt{A_1})\,[(-16\,h\beta D_1D_2+3(2+h^2\beta-2\,h\beta y)\sqrt{A_1}\,(D_1^2-D_2^2)\,]+$$

$$192\,h^2A_1^{\frac{9}{2}}D_3.\sin(y\sqrt{A_1})-6\,A_1^{\frac{3}{2}}.\cos(y\sqrt{A_1})\,[(6(n-1)\sqrt{A_1}\,Gr^2h\beta D_1(2+h^2\beta-2\,h\beta y)+2(n-1)\,Gr^2A_1^{\frac{3}{2}}D_1y$$

$$[(12-12\,h\beta y+3\,h^4\beta^2-6\,h^3\beta^2y+4\,h^2\beta(3+h^2\beta)]-6(n-1)\,Gr^2h^2\beta^2D_2+3(n-1)\,Gr^2A_1D_2[(12-8\,h\beta y+$$

$$3\,h^4\beta^2-4\,h^3\beta^2y+4\,h^2\beta(3+h^2\beta)]+3(n-1)\,h^2A_1^4(D_1^2+D_2^2)\,[2\sqrt{A_1}D_1y+3\,D_2]+32\,h^2A_1^3D_4]\} \quad (43)$$

The formula of u_1, u_2 and ψ_2 is a very long. The attendant constants D_3, D_4, D_5 and D_6 can be determinate by using the boundary conditions equations (37) and (40).

Finally, the perturbation solutions up to second order for *u* and ψ are given by

$$u = u_0 + We^2u_1 + We^4u_2 \quad (44)$$

$$\psi = \psi_0 + We^2\psi_1 + We^4\psi_2 \quad (45)$$

4. RESULTS AND DISCUSSION

In this section, the numerical and computational results are discussed for the problem of an incompressible non-Newtonian the peristaltic flow of a Carreau fluid model through porous medium under combined effects of MHD and wall properties through the graphical illustrations. The numerical evaluations of the analytical results and some important results are displayed graphically in figures 2 - 18. MATHEMATICA program is used to find out numerical results and illustrations. The analytical solutions of the momentum equation and temperature equation are obtained by using perturbation technique. All the obtained solutions are discussed graphically under the variations of various pertinent parameters in the present section. The trapping bolus phenomenon is also incorporated through sketching graphs of streamlines for various physical parameters.

Based on equation (44), figures 2 - 7 illustrates the effects of the parameters E_1, E_2, E_3, *We*, *Gr*, β, *M*, *Da*, ϕ and *n* on the velocity. Figure 2 illustrates the effects of the parameters E_1 and E_2 on the velocity distribution function *u* vs. y. It is found that the velocity profile *u* rising up with the increasing effects of both the parameters E_1 and E_2, when $|y|$ < 0.8643, and attains its maximum height at *y* = 0, the fluid velocity starts increasing and tends to be constant at the peristaltic wall $h(x)$ as specified by the boundary conditions. From figure 3 One can depict here that velocity decreases with increasing of E_3, while that velocity profile is rising up with increasing of the parameters *We*, when $|y|$ < 0.8643. Figure 4 contains the behavior of *u* under the variation of *Gr* and β, one can depict here that *u* go down with the increasing effects of both the parameters *Gr* and β, when $|y|$ < 0.8643. Figure 5 illustrates the effects of the parameters *M* and *Da* on velocity profile. One can depict here that velocity decreases with increasing of *Da*, while that velocity profile is rising up with increasing of *M*, when $|y|$ < 0.8643. Figure 6 show that velocity distribution decreases with the increasing of ϕ. Also at ϕ = 0.15, *u* > 0 when $|y|$ < 0.8643 and *u*(0.8643) = 0. At ϕ = 0.175, *u* > 0 when $|y|$ < 0.8417 and *u*(0.8417) = 0. At ϕ = 0.2, *u* > 0 when $|y|$ < 0.8191 and *u*(0.8191) = 0. And at ϕ = 0.225, *u* > 0 when $|y|$ < 0.7965 and *u*(0.7965) = 0, as specified by the boundary conditions. And Figure 7 show that velocity distribution decreases with the increasing of *n*.

ISSN 2347-3487

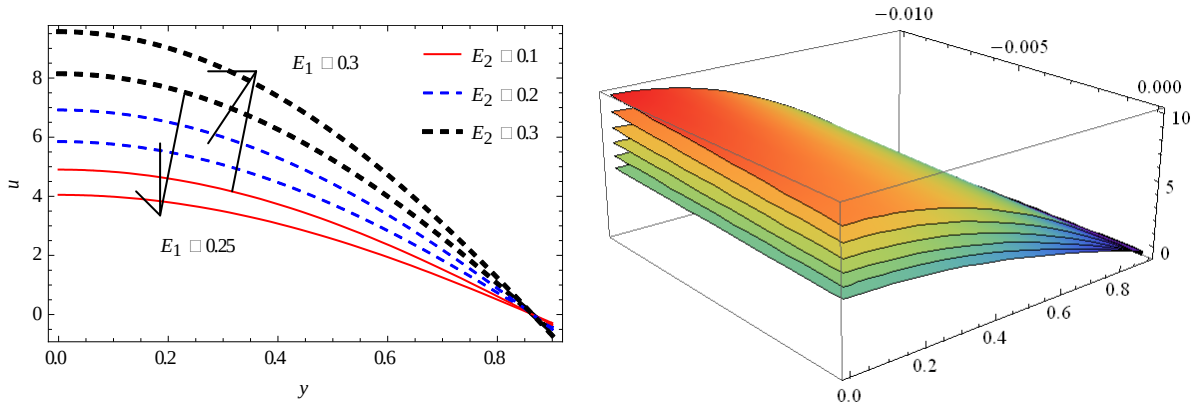

Figure2. Velocity profile for different values of E_1 and E_2 with

$x=0, t=0.1, We=0.05, n=0.5, E_3=0.1, Gr=1, \phi=0.15, \beta=1, Da=0.7, M=0.9$

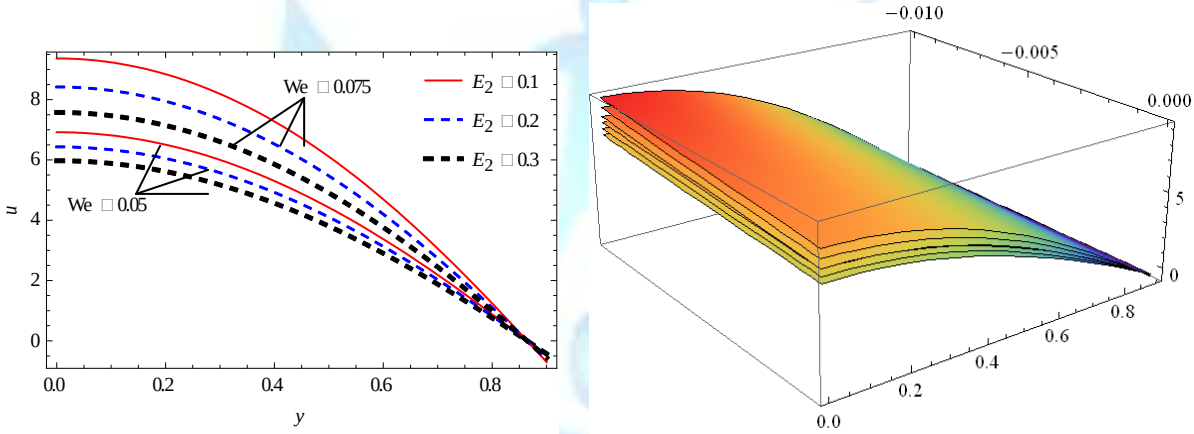

Figure3. Velocity profile for different values of *We* and E_3 with

$x=0, t=0.1, n=0.5, E_1=0.3, E_2=0.2, Gr=1, \phi=0.15, \beta=1, Da=0.7, M=0.9$

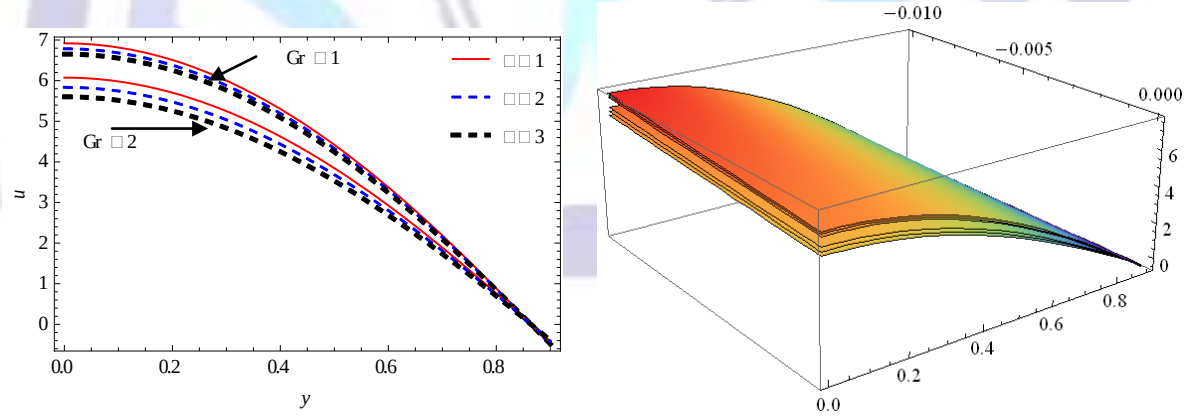

Figure4. Velocity profile for different values of Gr and β with

$x=0, t=0.1, We=0.05, n=0.5, E_1=0.3, E_2=0.2, E_3=0.1, \phi=0.15, Da=0.7, M=0.9$

ISSN 2347-3487

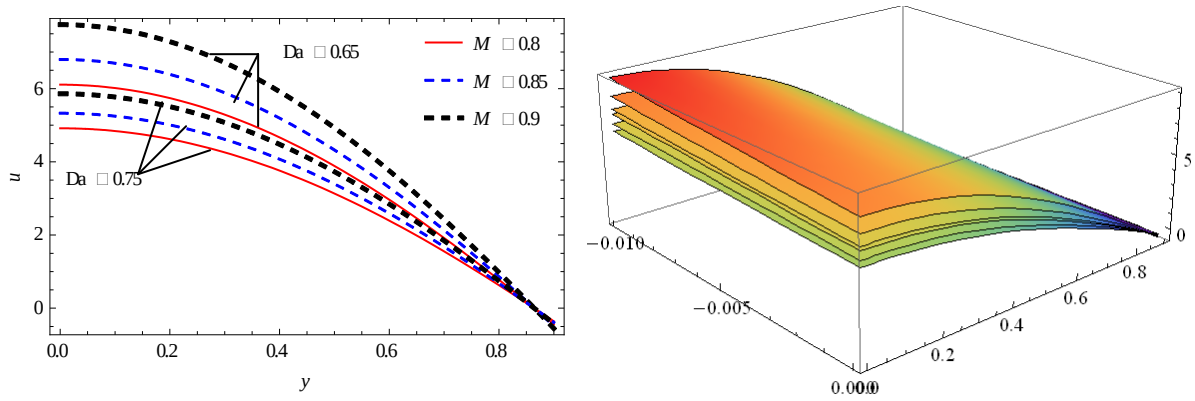

Figure5. Velocity profile for different values of *Da* and *M* with
$x = 0, t = 0.1, We = 0.05, n = 0.5, E_1 = 0.3, E_2 = 0.2, E_3 = 0.1, Gr = 1, \phi = 0.15, \beta = 1$

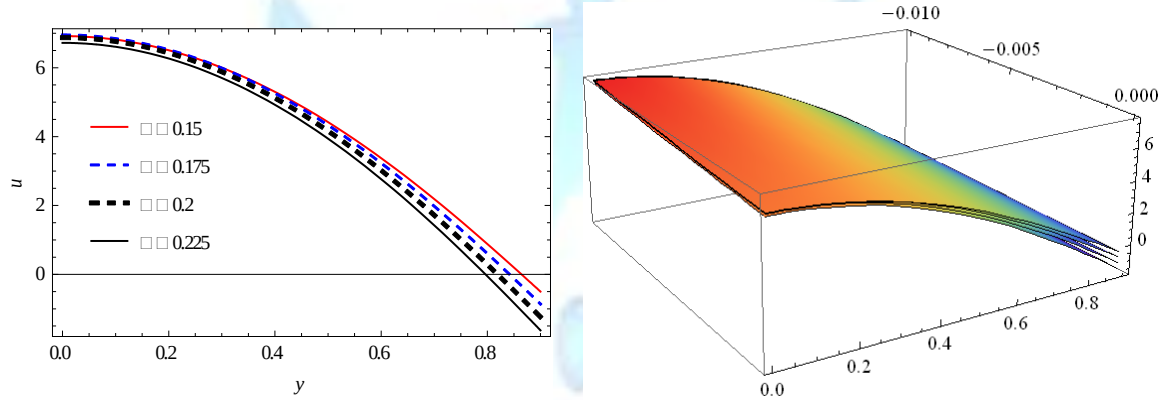

Figure6. Velocity profile for different values of ϕ with
$x = 0, t = 0.1, W = 0.5, n = 0.5, E_1 = 0.3, E_2 = 0.2, E_3 = 0.1, \beta = 1, Gr = 1, Da = 0.7, M = 0.9$

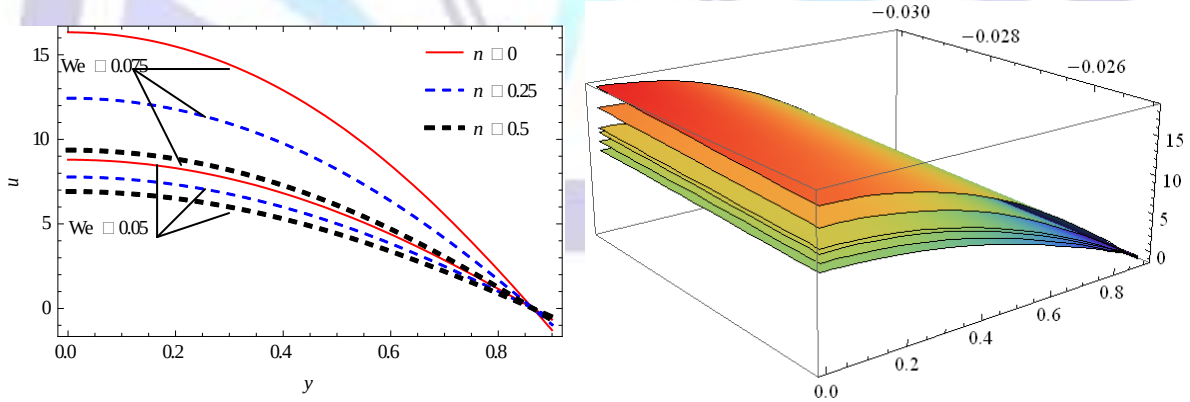

Figure7. Velocity profile for different values of *n* and *We* with
$x = 0, t = 0.1, E_1 = 0.3, E_2 = 0.2, E_3 = 0.1, \phi = 0.15, \beta = 1, Gr = 1, Da = 0.7, M = 0.9$

ISSN 2347-3487

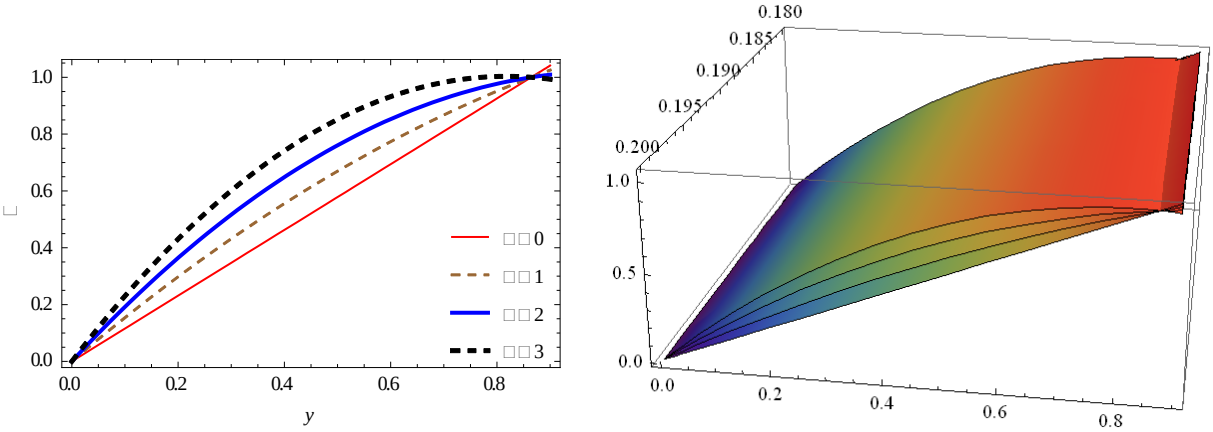

Figure8. Temperature distribution for different values of β with $x=0, t=0.1, \phi=0.15$

Based on equation (30), figure 8 shows that effects of the parameter β on the temperature distribution function θ. The temperature increases with the increase in β, when $|y|$ < 0.8643, and θ (0.8643) = 1 (at *y* = *h* = 0.8643) as specified by the boundary conditions.

5. TRAPPING PHENOMENON

The formation of an internally circulating bolus of fluid by closed streamlines is called trapping and this trapped bolus is pushed ahead along with the peristaltic wave.

Based on equation (45), the effects of E_1, E_2, E_3, *Gr*, β, *Da*, *M*, *We*, ϕ and *n* on trapping can be seen through Figures 9 - 18, it is observed that the bolus move near the side walls. Figure 9 show that the size of the trapped bolus increase with the increase in E_1. Figure 10 is plotted the effect of E_2 on trapping, the size of the trapped bolus increase with the increase in E_2. Figure 11 show that the size of the left trapped bolus increases with increase in E_3 where as the size of the right trapped bolus decreases with increase in E_3. The effect of Grashof number *Gr* on trapping is analyzed in Figure 12. It can be concluded that the size of the trapped bolus in the left side of the channel decreases when *Gr* increases where as it has opposite behavior in the right hand side of the channel. Figure 13 show that the size of the left trapped bolus decreases with increase in β where as the size of the right trapped bolus increases with increase in β. The influence of Darcy number *Da* on trapping is analyzed in Figure 14. It shows that the size of the trapped bolus decreases with increase in *Da*. Figure 15 show that influence of *M* on trapping. It shows that the size of the trapped bolus increases with increase in *M*. The influence of Weissenberg number *We* on trapping is analyzed in Figure 16. It shows that the size of the trapped bolus increases with increase in *We*. The effect of ϕ on trapping is analyzed in figure 17. We notice that the size of the trapped bolus increases with increase ϕ. And figure 18 show that the size of the trapped bolus decreases with increase in *n*.

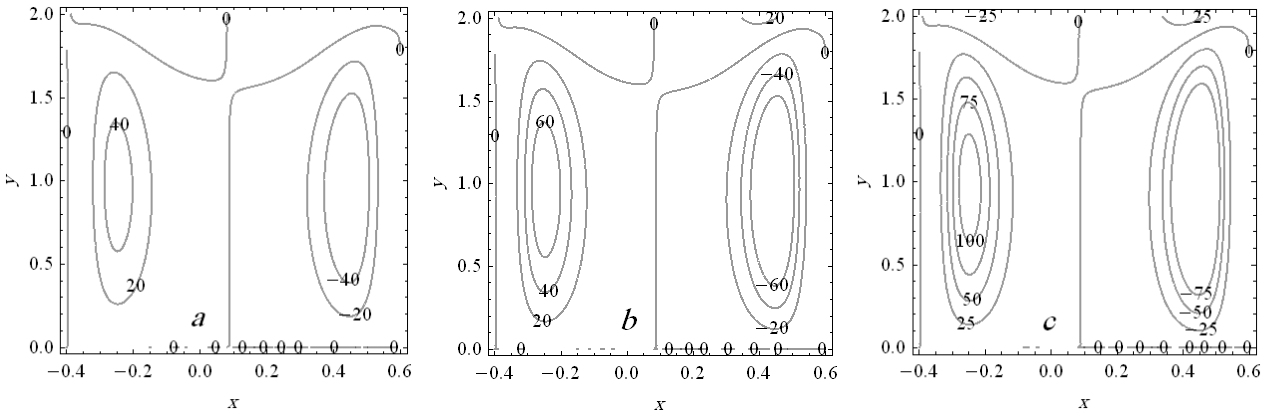

ISSN 2347-3487

Figure9. Graph of the streamlines for three different values of E_1; (a) E_1 = 0.25, (b) E_1 = 0.3 and (c) E_1 = 0.35 at
$t = 0.1, We = 0.05, n = 0.5, E_2 = 0.2, E_3 = 0.1, Da = 0.8, M = 0.9, Gr = 1, \phi = 0.15, \beta = 1$

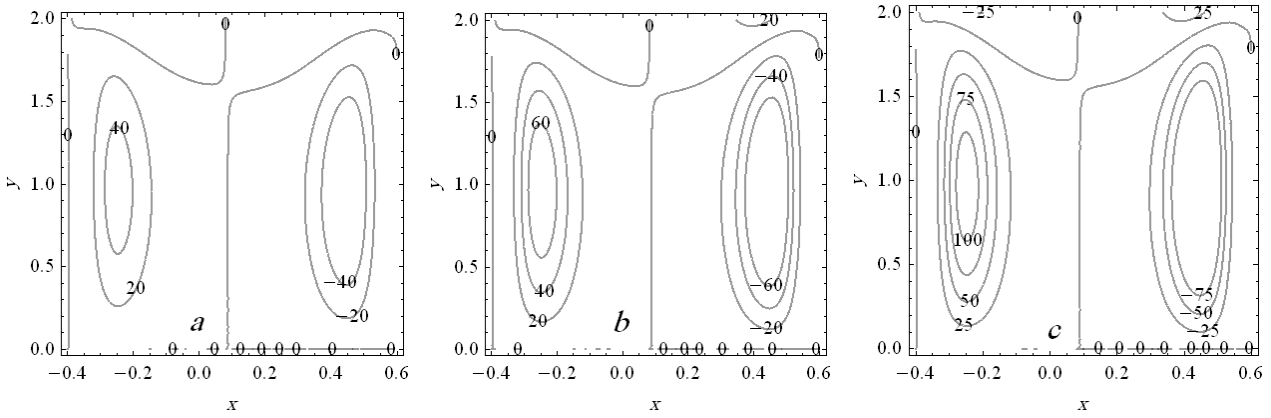

Figure10. Graph of the streamlines for three different values of E_2; (a) E_2 = 0.15, (b) E_2 = 0.2 and (c) E_2 = 0.25 at
$t = 0.1, We = 0.05, n = 0.5, E_1 = 0.3, E_3 = 0.1, Da = 0.8, M = 0.9, Gr = 1, \phi = 0.15, \beta = 1$

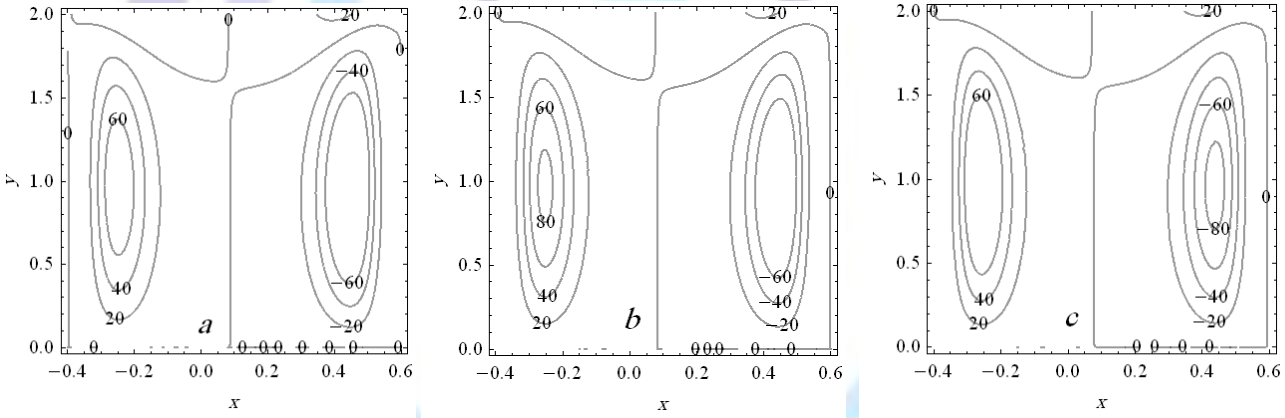

Figure11. Graph of the streamlines for three different values of E_3; (a) E_3 = 0.1, (b) E_3 = 0.2 and (c) E_3 = 0.3 at
$t = 0.1, We = 0.05, n = 0.5, E_1 = 0.3, E_2 = 0.2, Da = 0.8, M = 0.9, Gr = 1, \phi = 0.15, \beta = 1$

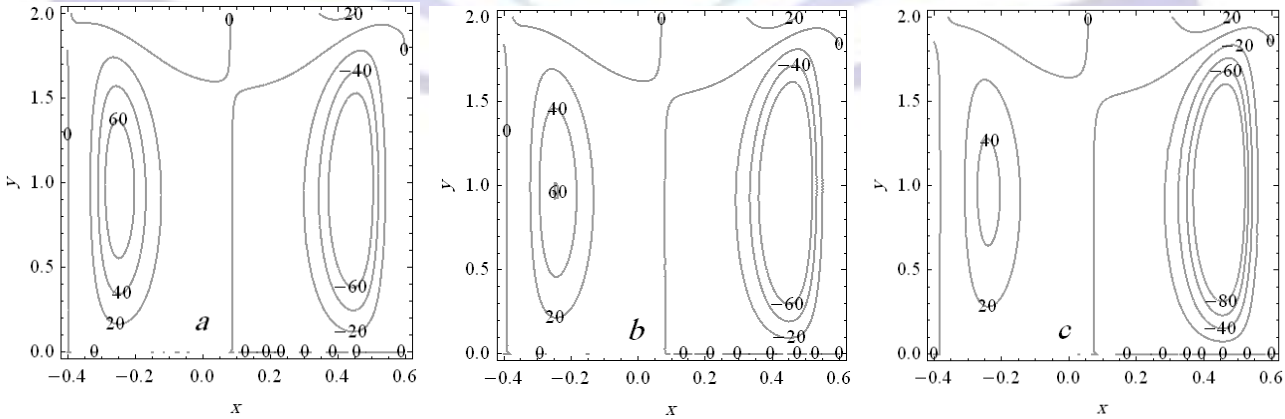

Figure12. Graph of the streamlines for three different values of *Gr*; (a) *Gr* = 1, (b) *Gr* = 2 and (c) *Gr* = 3 at
$t = 0.1, We = 0.05, n = 0.5, E_1 = 0.3, E_2 = 0.2, E_3 = 0.1, Da = 0.8, M = 0.9, \phi = 0.15, \beta = 1$

ISSN 2347-3487

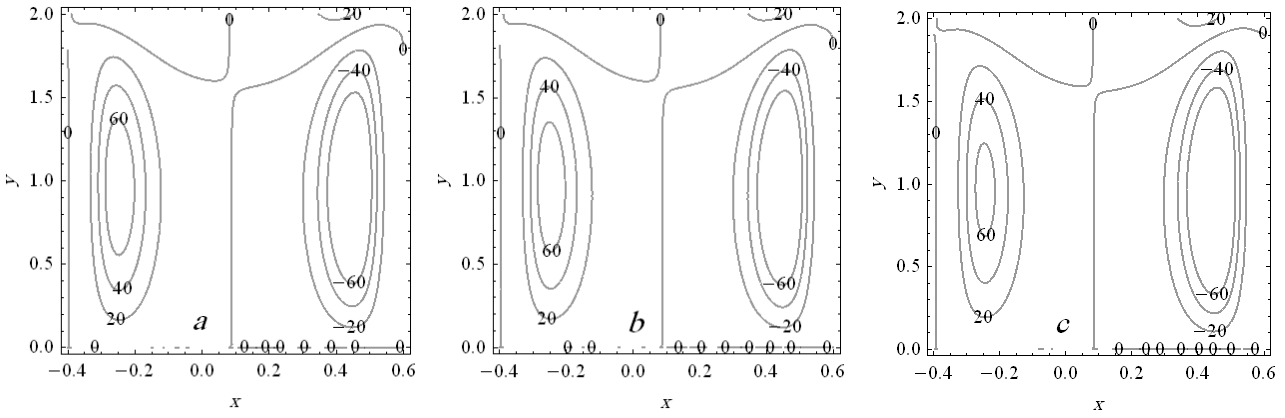

Figure13. Graph of the streamlines for three different values of β ; (a) β = 1, (b) β = 2 and (c) β = 4 at
$t = 0.1, We = 0.05, n = 0.5, E_1 = 0.3, E_2 = 0.2, E_3 = 0.1, Da = 0.7, M = 0.9, Gr = 1, \phi = 0.15$

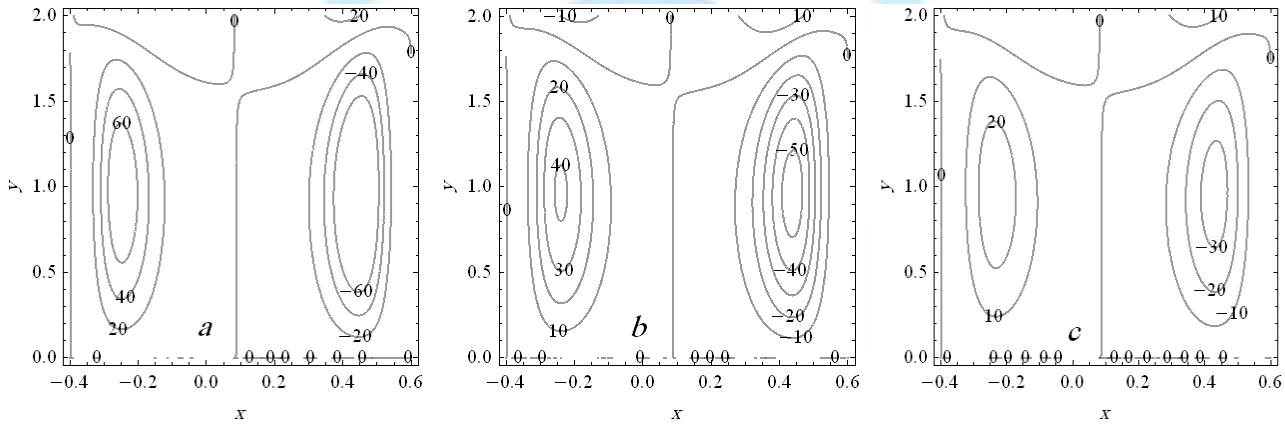

Figure14. Graph of the streamlines for three different values of *Da*; (a) *Da* = 0.8, (b) *Da* = 0.85 and (c) *Da* = 0.9 at
$t = 0.1, We = 0.05, n = 0.5, E_1 = 0.3, E_2 = 0.2, E_3 = 0.1, M = 0.9, Gr = 1, \phi = 0.15, \beta = 1$

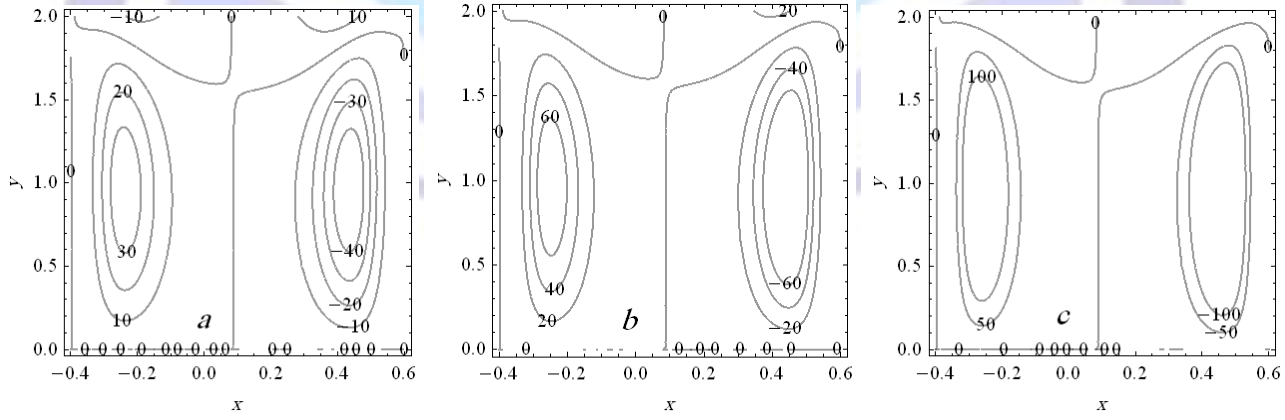

Figure15. Graph of the streamlines for three different values of *M*; (a) *M* = 0.8, (b) *M* = 0.9 and (c) *M* = 0.95 at
$t = 0.1, We = 0.05, n = 0.5, E_1 = 0.3, E_2 = 0.2, E_3 = 0.1, Da = 0.8, Gr = 1, \phi = 0.15, \beta = 1$

ISSN 2347-3487

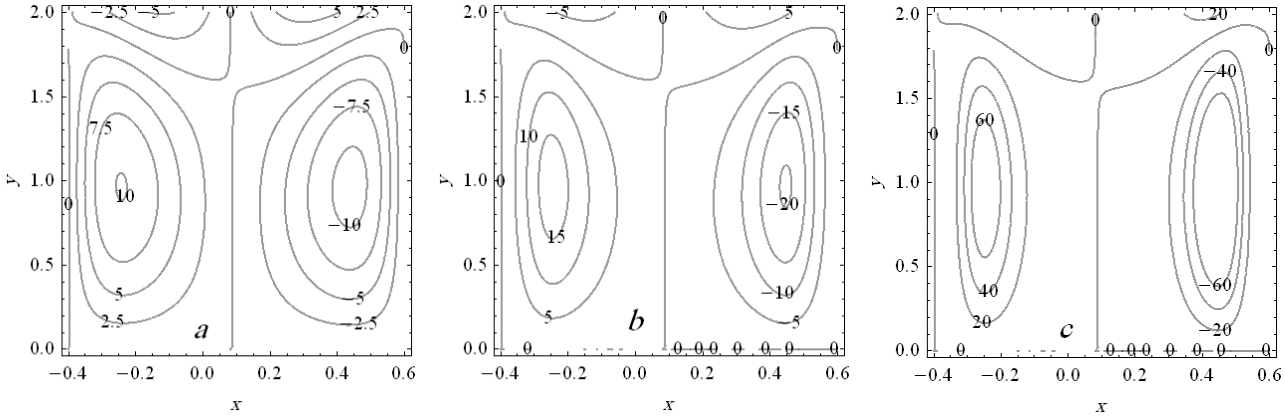

Figure16. Graph of the streamlines for three different values of *We*; (a) *We* = 0, (b) *We* = 0.025 and (c) *We* = 0.05 at
$t = 0.1, n = 0.5, E_1 = 0.3, E_2 = 0.2, E_3 = 0.1, Gr = 1, Da = 0.8, M = 0.9, \phi = 0.15, \beta = 1$

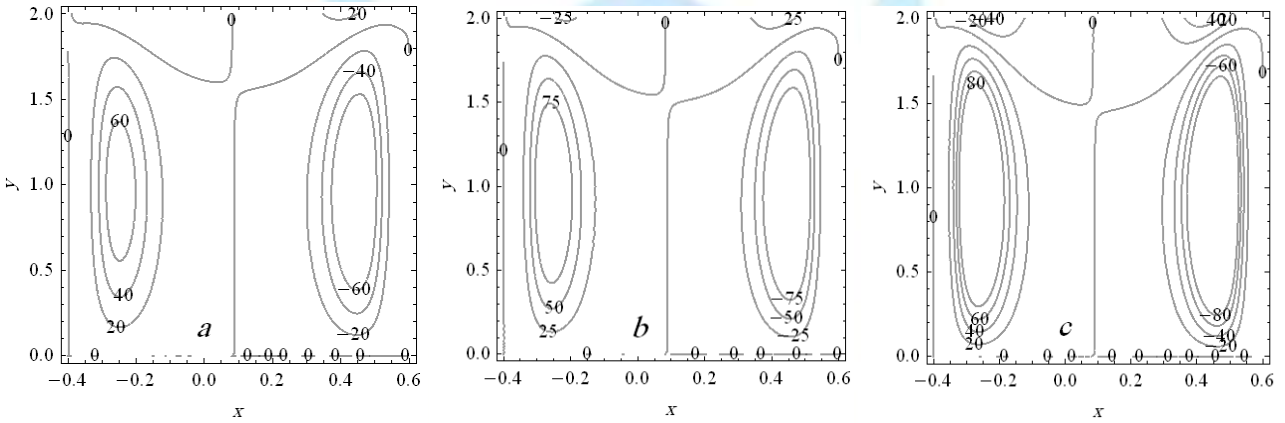

Figure17. Graph of the streamlines for three different values of ϕ ; (a) ϕ = 0.15, (b) ϕ = 0.175 and (c) ϕ = 0.2 at
$t = 0.1, We = 0.05, n = 0.5, E_1 = 0.3, E_2 = 0.2, E_3 = 0.1, Da = 0.8, M = 0.9, Gr = 1, \beta = 1$

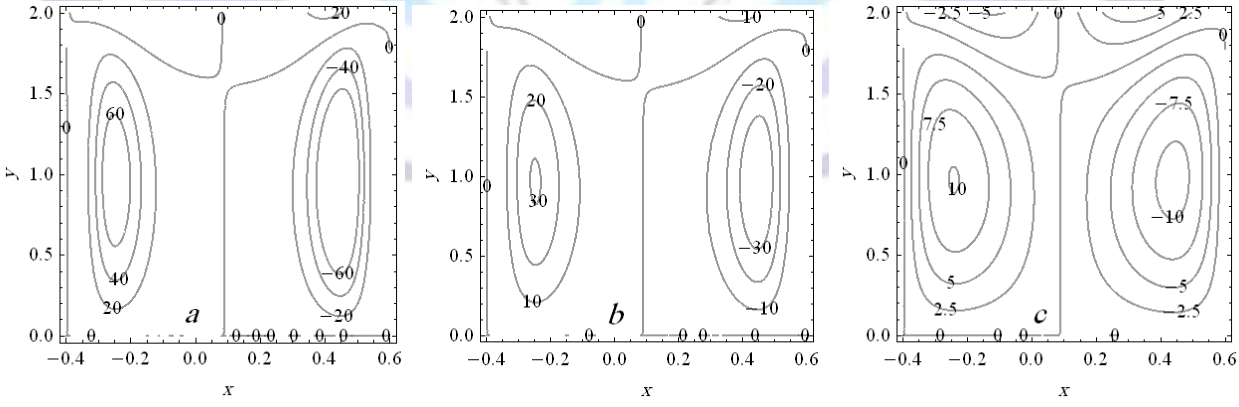

Figure18. Graph of the streamlines for four different values of *n*; (a) *n* = 0.5, (b) *n* = 0.75, and (c) *n* = 1 at
$t = 0.1, We = 0.05, E_1 = 0.3, E_2 = 0.2, E_3 = 0.1, Gr = 1, Da = 0.7, M = 0.9, \phi = 0.15, \beta = 1$

6. CONCLUDING REMARKS

The present study deals with the combined effect of MHD and wall properties on the peristaltic transport of a Carreau fluid in a two dimensional channel through porous medium. We obtained the analytical solution of the problem under long wavelength and low Reynolds number assumptions. The perturbation series in the Weissenberg number (*We* < 1) was

used to obtain explicit forms for velocity field and stream function per one wavelength. The results are analyzed for different values of pertinent parameters namely Grashof number, Darcy number, thermal conductivity, rigidity, stiffness, magnet and viscous damping forces of the channel wall through porous medium. From wall properties and type of fluid (Carreau), we observed that the bolus move near the side walls. The main findings can be summarized as follows:

1. The axial velocity increases with the increase in E_1, E_2, *We* and *M*, when $|y|$ < 0.8643. Further, the axial velocity decreases with increase in E_3, *Gr*, β, *Da*, ϕ and *n*.

2- The size of the trapped bolus increase with the increase in E_1, E_2, *M*, ϕ and *We*. While the size of the trapped bolus decreases with increase in *Da* and *n*.

3- The size of the left trapped bolus increases with increase in E_3 where as the size of the right bolus decreases with increase in E_3. And the size of the trapped bolus in the left side of the channel decreases when *Gr* and β increases where as it has opposite behavior in the right hand side of the channel.

4. The coefficient of temperature increases with increasing values of thermal conductivity.

REFERENCES

1. Latham TW, M.S. Thesis, MIT, *Cambridge, Massachussetts*, **1966**.
2. Shapiro AH, Jaffrin Y, Weinberg SL, *Journal of Fluid Mechanics*, **1969,** 37, 799-825.
3. Siddiqui AM, Schehawey WH, *Journal of Non Newtonian Fluid Mechanics*, **1994**, 53, 257-284.
4. Mishra M, Ramachardra Rao A, *ZAMP*, **2003**, 54, 532-550.
5. Subba Reddy MV, Ramachandra Rao A, Sreenadh S, *Int. J. Non-Linear Mech.,* **2007**, 42, 1153-1161.
6. Vajravelu K, Sreenadh S, Hemadri reddy R, Murugesan K, *International Journal of Fluid Mechanics Research*, **2009**, 36(3), 244-254.
7. Nadeem S, Safia Akram, *Communications Nonlinear Sci Numer Simulat*, **2010**, 15, 312-321.
8. Vajravelu K, Sreenadh S, Rajanikanth K, Chanhoon Lee, *Nonlinear Analysis, Real World Applications*, **2012**,13, 2804-2822.
9. Mishra M, Ramachandra Rao A, *Acta Mechanica*, **2004**,168, 35-39.
10. Hayat T, Nasir Ali, Zaheer Abbas**,** *Physics letters A***, 2008**, 370, 331-344.
11. Srivastava LM, Srivastava VP, *J. Fluid. Mech.* **1984**,122, 439-465.
12. Elshehawey EF, Eldabe NT, Elghazy EM, Ebaid A, *Applied Mathematics and Computation*, **2006**,182(1), 140-150.
13. Pandey SK, Chaube MK, *Communications in Nonlinear Science and Numerical Simulation*, **2011**, 16(9), 3591-3601.
14. Subba Reddy MV, Mishra M, Sreenadh S, Rao AR, *Journal of Fluids Engineering*, **2005**,127(4), 824-827.
15. Hemadri Reddy R, Kavitha A, Sreenadh S, Hariprabhakaran P, *Advances in applied Science Research*, **2005**, 2(2), 167-178.
16. Lakshminarayana P, Sreenadh S, Sucharitha G, *Advances in Applied Science Research*, **2012**, 3(5), 2890-2899.
17. Radhakrishnamacharya G, Srinivasulu Ch, *Computer Rendus Mecanique*, **2007**,335, 369-373.
18. Hayat T, Noreen S, *Computer Rendus Mécanique*, **2010**, 338, 518-528.
19. Mekheimer Kh, *Physics letters A*, **2008**, 371, 4271-4278.
20. Srinivas S, Gayathri R, Kothandapani M, *Computer Physics Communications*, **2009**,180, 2115-2122.
21. Abd-Alla AM, Yahya GA, Mahmoud SR, Alosaimi HS, *Meccanica*, **2012**, 47, 1455-1465.
22. Ebaid A, *Physics letters A*, **2008**, 372, 4493-4499.
23. Srinivas S, Kothandapani M, *Applied Mathematics and Computation*, **2009**, 213, 197-208.
24. Nadeem S, Akram S, *Communications in Nonlinear Science and Numerical Simulation*, **2010**, 15, 312-321.
25. Rajanikanth K, Sreenadh S, Rajesh yadav Y, Ebaid A, *Advances in applied Science Research*, **2010**, 3(6), 3755-3765.
26. Prasana Hariharan, Seshadri V, Rupak Banerjee, *Mathematical and Computer Modeling*, **2008**, 48, 998-1017.

27. Rajnikanth K, Rajesh yadav Y, Sreenadh S, *International Journal of Fluid Mechanics*, **2013**, 5(2), 81-96.
28. Wang Y, Hayat T, Ali N, Oberlack M, *Physics letters A*, **2008**, 387, 347-362.
29. Kothandapani M, Srinivas S, *Int. J Non-linear Mech*., **2008**, 43, 915-924.
30. Hayat T, Ahmad N, Ali N, *Communications in Nonlinear Science and Numerical Simulation*, **2008**, 13, 1581-1591.
31. Rathod VP, Pallavi Kulkarni, *Advances in applied Science Research*, **2011**, 2(3), 265-279.
32. Mokhtar A, Elnaby, Haroun MH, *Communication in Nonlinear Science and Numerical simulation*, **2008**, 13, 752-762.
33. Srinivas S, Gayathri R, Kothandapani M, *Computer Physics Communications*, **2009**, 180, 2116-2112.
34. Sreenadh S, Arun Kumar M, Srinivas S, *Advances in Applied Science Research*, **2013**, 4(6), 159-172.
35. Al-Khafajy DG, Abdulhadi AM, *Mathematical Theory and Modeling–IISTE*, **2014**, 4(9), 86-99.
36. Ali N, Hayat T, *Appl. Math. Comput*, **2007**, 193(2), 535-552.
37. Hayat T, Saleem N, Ali N, *Communications in Nonlinear Science and Numerical Simulation,* **2010**, 15(9), 2407-2423.
38. Carreau PJ, De Kee D, Daroux M, *Can. J. Chem. Eng*., **1979**, 57,135-141.